10. Kotenko A., Nikolaenko L., Lugova S. The computational model of the emergence and development of cavitation in torque flow pump // 4th International Meeting on Cavitation and Dynamic Problems in Hydraulic Machinery and Systems. 2011. P. 87–94.
11. Numerical Approach for Simulation of Fluid Flow in Torque Flow Pumps / Krishtop I., German V., Gusak A., Lugova S., Kochevsky A. // Applied Mechanics and Materials. 2014. Vol. 630. P. 43–51. doi: 10.4028/www.scientific.net/amm.630.43
12. Grabow G. Einfluss der Beschaufelung auf das Kennlinie Verhalten von Freistrompumpen // Pumpen und Verdichter. 1972. Issue 2. P. 18–21.

У даному дослідженні було розроблено нову суцільну конструкцію теплових труб для підвищення теплових характеристик. Вивчення кипіння у суцільній тепловій трубі досліджується для детальної інформації про зародження бульбашок. Експеримент проводився в суцільних теплових трубах з варіацією випарника (d) до співвідношення діаметра конденсатора (D). Значення d/D змінюються в 1/1; 1/2; 1/3 і 1/4. Теплове навантаження генерується на секції випарника з використанням DC-Power нагрівача на 30, 40 та 50 Вт. Технологія візуалізації була розроблена за допомогою прозорої скляної трубки, а знімки киплячих бульбашок були зроблені дзеркальною камерою. Нахил скляної труби становить 45° та інтегровано з модулем NI-9211 та c-DAQ 9271. Термопари K-типу встановлювалися на випарнику та конденсаторних секціях для вимірювання температури кипіння в суцільній тепловій трубі.

Виходячи з результатів, можна зазначити, що різні варіації співвідношення теплового навантаження та співвідношення діаметра (d/D) випарника та конденсатора впливають на розмір і форму киплячих бульбашок, а також температуру зародження на суцільній тепловій трубі. Коефіцієнт теплопередачі має тенденцію до збільшення при тепловому навантаженні 50 Вт та співвідношенні діаметра d/D=1/4

Ключові слова: візуалізація кип'ятіння, утворення бульбашок, конічна труба теплопоглинання, коефіцієнт випаровування до діаметра конденсатора

UDC 62-67
DOI: 10.15587/1729-4061.2018.133973

VISUALIZATION OF BUBBLES FORMATION ON THE BOILING PROCESS IN TAPERING HEAT PIPE WITH VARIATION OF EVAPORATOR TO CONDENSER DIAMETER RATIO

Sarip
Doctoral Student
Department of Mechanical Engineering
Ronggolawe Technology High School
Jalan. Campus Ronggolawe Blok B/I,
Cepu, Indonesia, 58312
Central Java Indonesia.
E-mail: hidayatullohsarip566@gmail.com
Sudjito Soeparman
Professor, Researcher*
E-mail: sudjitospn@ub.ac.id
Lilis Yuliati
Doctor of Mechanical Engineering, Researcher*
E-mail: lilis_y@ub.ac.id
Moch. Agus Choiron
Doctor of Mechanical Engineering, Researcher*
E-mail: agus_choiron@ub.ac.id
*Department of Mechanical Engineering
University of Brawijaya Malang
Jalan. Mayjend Haryono, 167, Malang, Indonesia, 65145

1. Introduction

Heat pipe is a technology that uses porous media in the form of wick, which serves as a path for the return of liquid fluid from the condenser to the evaporator. The basic principle Heat pipe uses two-phase flow, latent heat and capillary channel for working fluid circulation between heating and cooling areas with wick media. The structure, design and construction of wick had a strong influence on heat pipe performance and had a critical aspect in the manufacturing process.

The working system of heat pipe at a certain pressure, the liquid will evaporate, while the steam will also melt at a certain temperature, so that there will be pressure settings in the heat pipe which in turn will also regulate the working temperature and phase changes from liquid to vapor and vice versa. The capillary pressure in the wick will move fluid even against gravity due to the effect of capillarity.

Techniques enhancement heat transfer can be classified into two methods, which are active method and passive method. Generally, the heat pipe has three parts, namely the evaporator, adiabatic section and the condenser as dissipation of the heat. Various heat pipe design features had been developed to enhance the thermal performances. While the thermal performance of heat pipe challenges is well understood, the research was focused on boiling visualization to provide the phenomenon of nucleation form. Based on the phenomenon of nucleation form, it can be determined thermal performance evaluation.

2. Literature review and problem statement

Heat pipe is a passive device of heat transfer from the heat source at the evaporator to the heat sink as the dissipation of heat in a relatively long time span through the evaporation latent heat of the working fluid [1]. An experimental technique has been developed to simultaneously visualize the evaporation process and measure the evaporator resistances of a flat-plate heat pipe [2–5].

Visualization study of vapor formation regimes during capillary-fed boiling in sintered-powder heat pipe wicks [6] provided a detailed indication of the fundamental vapor-formation regimes occurring at different heat fluxes and allows correlation of the evaporation/boiling mechanisms to thermal performance trends and surface modifications.

Visualization experiments were conducted to measure the performances of heat pipes by copper mesh with various surface wettability in the condenser and the evaporator [7]. In the next study, visualization of the condensation process was conducted on flat-plate heat pipes [8].

In the work [9], visualization of the evaporation/boiling process and thermal measurements of operating horizontal transparent heat pipes by glass tube and water as the working fluid was studied. Study results indicated that nucleate boiling was prompted for a wick having a fine 200-mesh bottom layer.

In the other study, inclination angle affects the thermal efficiency of the heat pipe on working fluid copper using Nano fluid [10]. The studied heat pipe with an inclination angle of 45° produces the highest thermal performance [11]. The heat pipe design is developed to provide the performance, and heat transfer improvement. Various designs of heat pipe had been investigated but the operation the heat pipe requires a fan to assist the heat dissipation process due to limitation of condenser section as heat dissipation, therefore it effected to high cost design.

In this study, the tapering heat pipe is investigated to enhance the thermal performances. The condenser section is larger than the evaporator section to provide the balancing of heat source and heat sink and continuous circulation. The tapering heat pipe does not require a fan because of different evaporator area and condenser. Boiling visualization in the tapering heat pipe is measured to provide the detailed information of bubbles nucleation.

3. The aim and objectives of the study

The aim of this study is to investigate the characteristics of bubbles formation on the boiling process in the tapering heat pipe with variation of the evaporator to condenser diameter ratio through visualization. The tapering heat pipe positioned at an inclination angle of 45° was set to provide the purpose.

To accomplish the set aim, the following tasks were set:

– to find the shape and size of the bubbles phenomenon at various heat loads and variation of the evaporator to condenser diameter ratio;

– to find the heat transfer coefficient and thermal resistance at various heat loads and variation of the evaporator to condenser diameter ratio.

4. Material, methods and model of research

Tapering heat pipes are made of a glass tube with a diameter ratio d/D=1/1, 1/2, 1/3 and 1/4, d is the outside diameter of the evaporator, d is constant =10 mm, and D is the condenser outside diameter. The length of the tapering heat pipe is 200 mm. Screen mesh wick serves as the axis of the capillary to return liquid from the condenser to the evaporator. The condenser ends insert a working fluid into the heat pipe tapering. Wick heat pipe of the mesh screen wire diameter in the form of 56.5μm single array with the number 67.416 per mm. Screen mesh wick made of stainless steel wire with a thermal conductivity of 40 W/(m·K), in the form of rolls following the shape of the tapering heat pipe so that the shape layer with a screen of 100 mesh. Its operation condition is room temperature and airtight during to the experiment with 100 ml of water Aqua as a working fluid. The heat source is used DC-Power supply to the condenser section. The design of the tapering heat pipe made of glass tube can be seen in Fig. 1 and the experimental set-up on tapering heat pipes with an inclination position 45° fixed can be seen in Fig. 2.

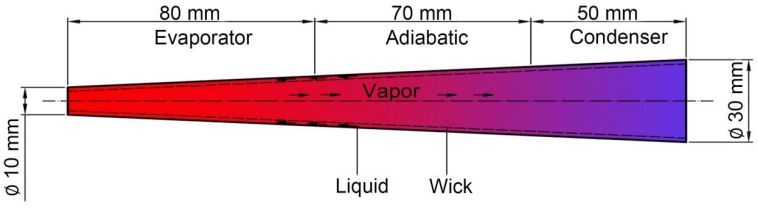

Fig. 1. Tapering heat pipe from glass tube with a diameter ratio d/D=1/3 (d=10 mm, D=30 mm) ø

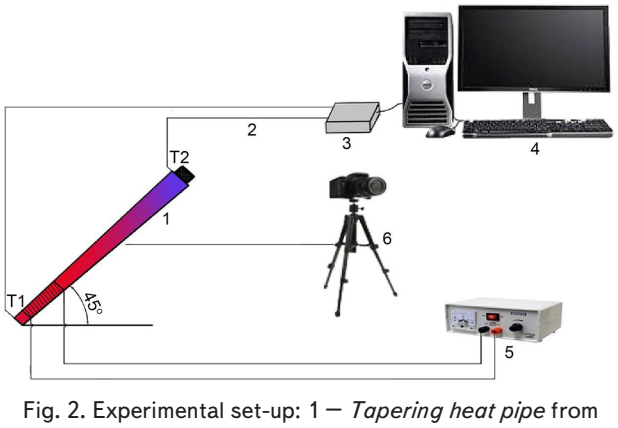

Fig. 2. Experimental set-up: 1 – *Tapering heat pipe* from glass tube; 2 – Thermocouple (T1, T2); 3 – 9171=c-DAQ and NI 9211- Module; 4 – Computer unit; 5 – Heater DC-Power Supply; 6 – SLR Camera

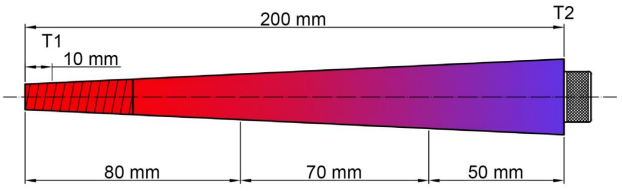

Fig. 3. Thermocouple positions

Tapering heat pipe testing was done by measuring the temperature at two points with the thermocouple positions of 10 mm, and 200 mm with the variation of the heat load of 30 W, 40 W and 50 W as T1 and T2 in Fig. 3. The variation of the heat load is taken because thermal yield at device several electronic average 30 W to 130 W. The tapering heat pipe is used in the electronic cooling system. One end of the tapering heat pipe is used as an evaporator, wires heater (flexible heater) is wound on the side of the evaporator which serves as a heat source and the condenser serves for heat dissipation. Heat source (Q) of the DC-power supply provides heat energy to the tapering heat pipe. K-type thermocouples are installed at two points to measure the boiling temperature distribution associated with data acquisition, 9171 c-DAQ and module NI-9211. The visualization is conducted by using a transparent glass tube no isolation and heat loss ignored so easy to images of boiling bubbles were captured by SLR camera. The heat flux is the evaporator section (q_e) was calculated by the equation (1) and the temperature of the inside and outside walls of the tapering heat pipe was calculated by the equation (2).

$$q_e = \frac{Q}{(2\pi r_0 L_e)}, \quad (1)$$

$$T_i = T_0 \frac{q_e r_0}{\lambda_w} ln \frac{r_i}{r_0}, \quad (2)$$

where Q is heat load, r_0 and r_i the radius of the outer and inner tapering heat pipes, L_e is the length of the evaporator, T_i and T_0 is the temperature of the inside and outside walls of tapering heat pipes and λ_w is the thermal conductivity of the glass tube. The coefficient of heat transfer from the evaporator can be calculated through a comparison between the heat flux at the evaporator with the temperature decrease ΔT by the equation (3). While thermal resistance can be calculated by the equation (4).

$$h_e = \frac{q_e}{\Delta T}, \quad (3)$$

$$R = \frac{T_{hot} - T_{cool}}{Q}. \quad (4)$$

5. Research results of the effect of the evaporator-condenser diameter ratio at various heat load on the bubble size, heat transfer coefficient and thermal resistance

a. Heat load of 30 Watt

The visualization results with heat load 30 W of variety of the evaporator-condenser diameter ratio are showed at Fig. 4. The boiling bubbles are occurs on the evaporator section. The bubbles visualization results are explained at discussion section.

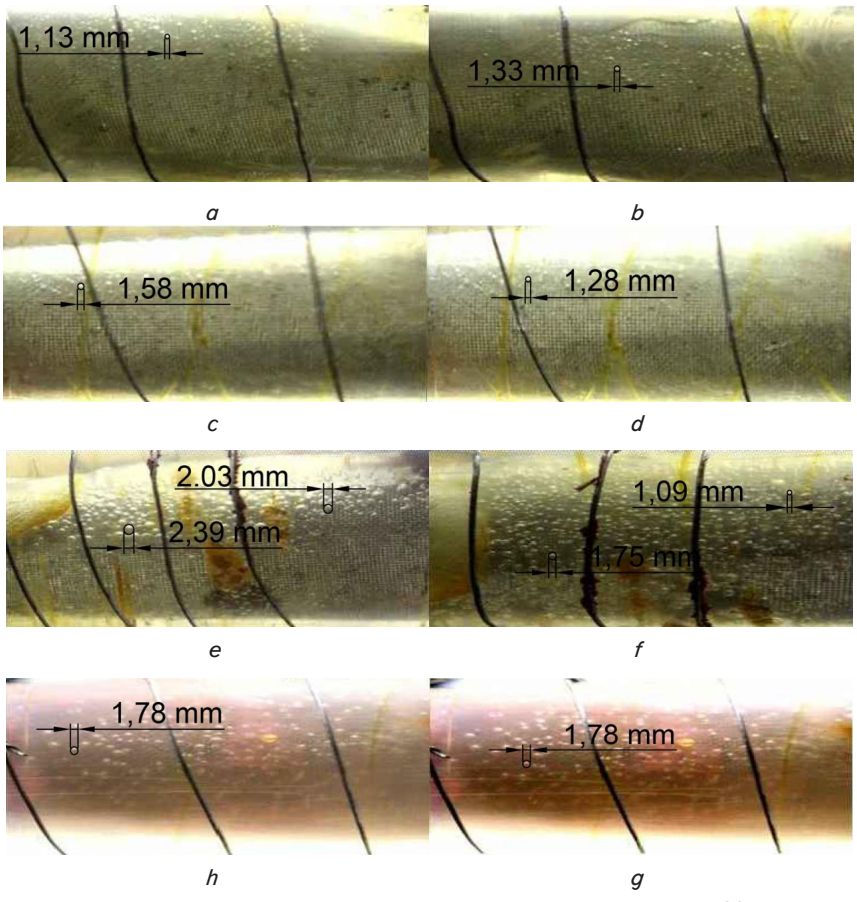

Fig. 4. Bubbles shape of the tapering heat pipe at a heat load of 30 W:
a – Evaporator to condenser diameter ratio (d/D)=1/1, q_e=9,952 kW/m^2;
b – Evaporator to condenser diameter ratio (d/D)=1/1, q_e=11,942 kW/m^2;
c – Evaporator to condenser diameter ratio (d/D)=1/2, q_e=9,952 kW/m^2;
d – Evaporator to condenser diameter ratio (d/D)=1/2, q_e=11,942 kW/m^2;
e – Evaporator to condenser diameter ratio (d/D)=1/3, q_e=9,952 kW/m^2;
f – Evaporator to condenser diameter ratio (d/D)=1/3, q_e=11,942 kW/m^2;
h – Evaporator to condenser diameter ratio (d/D)=1/4, q_e=9,952 kW/m^2;
g – Evaporator to condenser diameter ratio (d/D)=1/4, q_e=11,942 kW/m^2

b. Heat load of 40 Watt

The visualization results with heat load 40 W of variety of the evaporator-condenser diameter ratio are showed at Fig. 5. The boiling bubbles are occurs on the evaporator section. The bubbles visualization results are explained at discussion section.

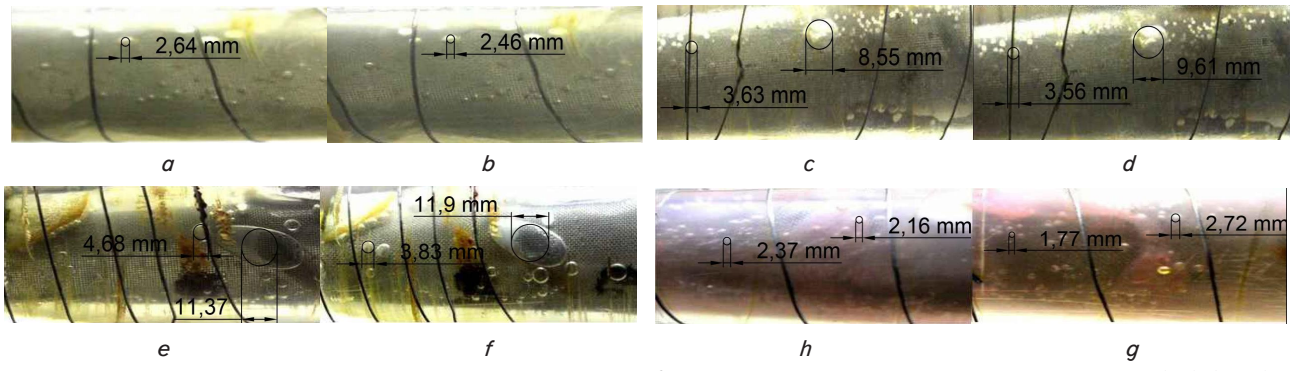

Fig. 5. Bubbles shape of the tapering heat pipe at heat load of 40 W: *a* – Evaporator to condenser diameter ratio (*d*/*D*)=1/1, q_e=13,933 kW/m^2;*b* – Evaporator to condenser diameter ratio (*d*/*D*)=1/1, q_e=15,923 kW/m^2; *c* – Evaporator to condenser diameter ratio (*d*/*D*)=1/2, q_e=13,933 kW/m^2; *d* – Evaporator to condenser diameter ratio (*d*/*D*)=1/2, q_e=15,923 kW/m^2; *e* – Evaporator to condenser diameter ratio (*d*/*D*)=1/3, q_e=13,933 kW/m^2; *f* – Evaporator to condenser diameter ratio (*d*/*D*)=1/3, q_e=15,923 kW/m^2; *h* – Evaporator to condenser diameter ratio (*d*/*D*)=1/4, q_e=13,933 kW/m^2; *g* – Evaporator to condenser diameter ratio (*d*/*D*)=1/4, q_e=15,923 kW/m^2

c. Heat load of 50 Watt

The visualization results with heat load 50 W of variety of the evaporator-condenser diameter ratio are showed at Fig. 6. The boiling bubbles are occurs on the evaporator section. The bubbles visualization results are explained at discussion section.

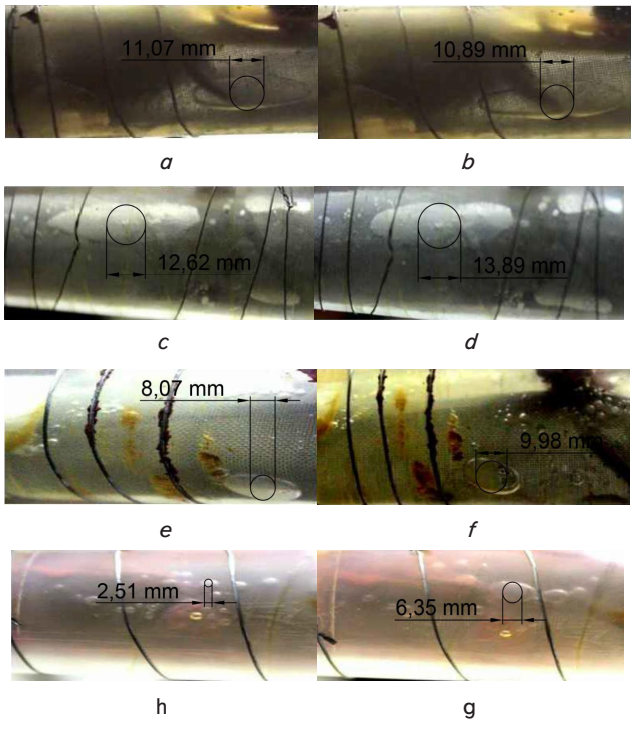

Fig. 6. Bubbles shape of the tapering heat pipe at heat load of 50 W: *a* – Evaporator to condenser diameter ratio (*d*/*D*)=1/1, q_e=17,914 kW/m^2; *b* – Evaporator to condenser diameter ratio (*d*/*D*)=1/1, q_e=19,904 kW/m^2; *c* – Evaporator to condenser diameter ratio (*d*/*D*)=1/2, q_e=17,914 kW/m^2; *d* – Evaporator to condenser diameter ratio (*d*/*D*)=1/2, q_e=19,904 kW/m^2; *e* – Evaporator to condenser diameter ratio (*d*/*D*)=1/3, q_e=17,914 kW/m^2; *f* – Evaporator to condenser diameter ratio (*d*/*D*)=1/3, q_e=19,904 kW/m^2; *h* – Evaporator to condenser diameter ratio (*d*/*D*)=1/4, q_e=17,914 kW/m^2; *g* – Evaporator to condenser diameter ratio (*d*/*D*)=1/4, q_e=19,904 kW/m^2

d. Heat flux and heat transfer coefficient

The heat transfer coefficient proces and heat flux on the tapering heat pipe of vareaty of the evaporator-condenser diameter ratio are showed at Fig. 7. The result heat flux and heat transfer coefficient are explained at discussion section.

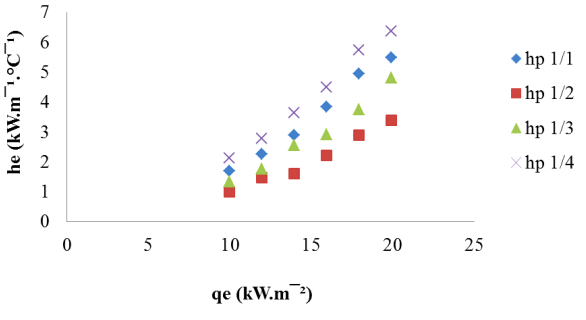

Fig.7. Heat transfer coefficient by heat flux

e. Thermal Resistance

The thermal resistance on the tapering heat pipe of vareaty of the evaporator-condenser diameter ratio are showed at Fig. 8. The result thermal resistance are explained at discussion section.

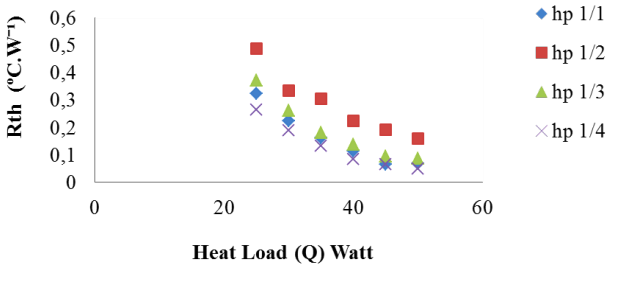

Fig. 8. Thermal resistance by heat load

6. Discussion of the research results of the effect of evaporator-condenser diameter ratio at various heat load on the bubble size, heat transfer coefficient and thermal resistance

Fig. 4 shows grow up and bubbles shape with variation of the evaporator-condenser diameter ratio and heat flux

enhancement of the inclined 45° on the tapering heat pipe. The phenomenon in Fig. 4, *a–d* occurs on the screen mesh wick surface of the heat flux 9,952 kW/m^2 to begin formation of nucleate bubbles on the screen mesh wick surface and heat flux 11,942 kW/m^2 bubbles number more increasing. Nucleate bubble is vapor bubbles occur at solid surface. The nucleate bubbles begin to disperse partly on the screen mesh wick surface by different size and shape. Fig. 4, *e–g* shows small bubbles occurred evenly by uniform size and shape on the screen mesh wick surface compared bubbles on the diameter ratio (d/D)=1/1. The phenomenon is indicated that the heat transfer process occurs better because the heat transfer coefficient, heat flux enhancement and thermal resistance decreased so that thermal performance increased.

The boiling phenomenon in Fig. 5, *a*, *b* is with variation of the heat load of 40 W generated bubbles shape larger size occurred between heat flux 13,933 kW/m^2 and heat flux 15,923 kW/m^2 at the long pipe. Fig. 5, *c–f* shows the boiling bubbles dispersed with different size and shape at the long pipe. Fig. 5 c is shows the bubbles less number and large size because of the small bubbles coalition. Bubbles number tends to increase as heat load increased, bubbles large size collapse prompt and rapidly leave the screen mesh wick surface in the form of vapor to then evaporation. Bubbles size in Fig. 5, *h*, *g* is less and uniform than in Fig. 5, *a–f* shows diameter ratio value increased not always generated large bubbles because different evaporator section and condenser area large.

The boiling phenomenon in Fig. 6, *a*, *b* is with variation of the heat load of 50 W, bubbles shape generated at condition is the big bubbles size and less number occurred at heat flux 17,914 kW/m^2 and heat flux 19,904 kW/m^2 in the long pipe. Fig. 6, *b*, *c* shows that the boiling bubbles occurred with different size and shape in the long pipe and tend the same with Fig. 5, *a–f*. Boiling bubbles in Fig. 6, *h*, *f* show the uniform size and shape but less bubbles size is larger caused rapidly collapse bubbles in the form of vapor then occur evaporation. Nucleate temperature is heat load of 50 Watt occurred faster compared with heat load of 30 W and 40 W because the heat transfer coefficient, heat flux increased and thermal resistance decreased so thermal performance enhancement. Bubbles shape and size change with variation of the d/D and heat load because existence different section area evaporator and condenser. Section area of the condenser is large and heat load increase cause rapid heat dissipation and vapor generated enhance. Vapor generated increase causes bubbles shape and size changed.

The feature of the proposed solutions is the new design of the tapering heat pipe with certain advantages without a fan the condenser section to lower cost. Future developments are excellent for electronic device coolers.

The effects of heat load on the heat transfer coefficient with variation of the evaporator to condenser diameter ratio is shown in Fig. 7. The diameter ratio value is increased result heat transfer coefficient and heat flux decreased but on diameter ratio 1/4 enhancement. This shows that the diameter ratio of 1/4 has conformity section area evaporator and condenser cause continue evaporation-condensation circulation so result heat transfer coefficient enhance.

The advantages of this research compared to similar ones is the increase of the heat transfer coefficient and heat flux on the diameter ratio of 1/4 because the evaporation-condensation process occurs continuously. This tapering heat pipe is without a fan, unlike another design of the heat pipe as a flat heat pipe, straight tube, circular tube etc.

The thermal resistance on the tapering heat pipe is the evaporator and condenser diameter ratio with various heat loads shown in Fig. 8. Diameter ratio d/D is as an independent variable and heat load is a dependent variable. Diameter ratio value is increased with the rise of the heat load result resistance thermal enhance but on the diameter ratio of 1/4 decreased. This shows that the diameter ratio of 1/4 has conformity section area evaporator and condenser cause continue evaporation-condensation circulation so result resistance thermal decreased. Heat transfer coefficient and thermal resistance change with variation of the d/D and heat load because temperature different ΔT small relatif between evaporator and condenser. The condenser section and heat load increasely vapor generated and gravitation force enlarged. The heat load and diameter ratio are affect heat transfer coefficient value and thermal resistance on the tapering heat pipe.

The shortcomings of the research are not installed pressure gauge on the evaporator section and condenser for measure work pressure. The restrictions can be imposed on the use of the results of the evaporator to condenser diameter ratio and various heat loads.

Can be the development of this research is flow boiling and pool boiling in the tapering heat pipe. The difficulties can be in trying to develop this research in these areas in the manufacturing process of the tapering heat pipe.

7. Conclusions

The visualization experiment result shows the evaporator to condenser diameter ratio and heat load effect on the boiling phenomenon as follows:

1. The bubbles shape and size are variation generated at various heat loads and variation of evaporator to condenser diameter ratio. Bubbles small disperse and group with quality is less clear occur at low heat load and evaporator to condenser little diameter ratio. Various heat loads and bigger ratio are generated of small bubbles grouping and there are greater ones with quality is clear.

2. Heat transfer coefficient enhanced and thermal resistance decreased for increasing heat load and grow diameter ratio.

References

1. Rao R. V., More K. C. Optimal design of the heat pipe using TLBO (teaching–learning-based optimization) algorithm // Energy. 2015. Vol. 80. P. 535–544. doi: 10.1016/j.energy.2014.12.008
2. Visualization and thermal resistance measurement for the sintered mesh-wick evaporator in operating flat-plate heat pipes / Liou J.-H., Chang C.-W., Chao C., Wong S.-C. // International Journal of Heat and Mass Transfer. 2010. Vol. 53. P. 7-8. P. 1498–1506. doi: 10.1016/j.ijheatmasstransfer.2009.11.046

3. Wong S.-C., Liou J.-H., Chang C.-W. Evaporation resistance measurement with visualization for sintered copper-powder evaporator in operating flat-plate heat pipes // International Journal of Heat and Mass Transfer. 2010. Vol. 53, Issue 19-20. P. 3792–3798. doi: 10.1109/impact.2009.5382185
4. Wong S.-C., Lin Y.-C. Effect of copper surface wettability on the evaporation performance: Tests in a flat-plate heat pipe with visualization // International Journal of Heat and Mass Transfer. 2011. Vol. 54, Issue 17-18. P. 3921–3926. doi: 10.1016/j.ijheatmasstransfer.2011.04.033
5. Wong S.-C., Lin Y.-C., Liou J.-H. Visualization and evaporator resistance measurement in heat pipes charged with water, methanol or acetone // International Journal of Thermal Sciences. 2012. Vol. 52. P. 154–160. doi: 10.1016/j.ijthermalsci.2011.09.020
6. Weibel J. A., Garimella S. V. Visualization of vapor formation regimes during capillary-fed boiling in sintered-powder heat pipe wicks // International Journal of Heat and Mass Transfer. 2012. Vol. 55, Issue 13-14. P. 3498–3510. doi: 10.1016/j.ijheatmasstransfer.2012.03.021
7. Wong S.-C., Cheng H.-S., Tu C.-W. Visualization experiments on the performance of mesh-wick heat pipes with differing wick wettability // International Journal of Heat and Mass Transfer. 2017. Vol. 114. P. 1045–1053. doi: 10.1016/j.ijheatmasstransfer.2017.06.107
8. Wong S.-C., Tseng H.-H., Chen S.-H. Visualization experiments on the condensation process in heat pipe wicks // International Journal of Heat and Mass Transfer. 2014. Vol. 68. P. 625–632. doi: 10.1016/j.ijheatmasstransfer.2013.09.069
9. Wong S.-C., Kao Y.-H. Visualization and performance measurement of operating mesh-wicked heat pipes // International Journal of Heat and Mass Transfer. 2008. Vol. 51, Issue 17-18. P. 4249–4259. doi: 10.1016/j.ijheatmasstransfer.2008.01.022
10. Application of nanofluid in an inclined mesh wicked heat pipes / Wang P.-Y., Chen X.-J., Liu Z.-H., Liu Y.-P. // Thermochimica Acta. 2012. Vol. 539. P. 100–108. doi: 10.1016/j.tca.2012.04.011
11. Senthilkumar R., Vaidyanathan S., Sivaraman B. Effect of Inclination Angle in Heat Pipe Performance Using Copper Nanofluid // Procedia Engineering. 2012. Vol. 38. P. 3715–3721. doi: 10.1016/j.proeng.2012.06.427